Innovation of Orthopedics and Implant
-Wisdom Academic Press

4D-Printed Shape Memory Alloy Bone Scaffolds for Dynamic Adaptation in Defect Repair

Abstract

This study developed 4D printed temperature-responsive NiTi scaffolds for dynamic bone defect repair. Medical-grade NiTi (55.8 wt% Ni) was laser powder bed fused into triply periodic minimal surface structures with gradient porosity (65-80%). Scaffolds exhibited phase transformation temperatures (Af=37.2 ° C, Ms=24.8 ° C) enabling physiological deployment. Elastic modulus transitioned from 2.8 ± 0.3 GPa at 20 ° C to 0.85 ± 0.12 GPa at 45 ° C, matching cortical-to-cancellous bone properties. Scaffolds achieved 98.2% shape recovery within 45 seconds, generating 12.5 ± 2.3 MPa recovery stress. In vitro results showed 4.2-fold RUNX2 upregulation and 8.9-fold increased proliferation versus static controls. Calvarial defect models demonstrated superior regeneration with 85.3 ± 6.8% new bone volume at 12 weeks versus 68.5 ± 7.2% for static scaffolds. Real-time strain mapping revealed 40% stress concentration reduction during adaptation. These findings establish 4D printed NiTi scaffolds as transformative for minimally invasive bone treatment, offering personalized adaptation through synchronized mechanical-biological stimulation.

Keywords:4D printing;Shape memory alloy;NiTi scaffold;Temperature-responsive;Bone regeneration

Thandiwe Dlamini*
Email: td.orthoinnov@yahoo.com
Affiliation: Mbabane Orthopedic Research Hub, King Mswati III Avenue, H100 Mbabane, Eswatini

1. Introduction

Bone defects from trauma, infection, tumors, and congenital abnormalities pose significant orthopedic challenges. Traditional treatments (autografts/allografts) face limitations including donor site morbidity and availability. While 3D printing creates customized scaffolds, these static structures lack dynamic adaptation capabilities needed for complex defects and bone regeneration.

Four-dimensional (4D) printing adds time dimension, enabling structures to change shape/properties under environmental stimuli [1]. This technology combines additive manufacturing flexibility with smart materials, particularly shape memory alloys (SMAs), offering scaffolds capable of controlled post-implantation deformation for enhanced surgical outcomes and tissue regeneration.

Nickel-titanium (NiTi) alloys are ideal for 4D printed bone scaffolds due to biocompatibility, mechanical properties, and temperature responsiveness [2]. NiTi exhibits shape memory effects and superelasticity, recovering original shape when heated above transformation temperature. Their elastic moduli match human bone, reducing stress shielding while providing excellent corrosion resistance and fatigue life.

Current fabrication limitations include creating porous architectures with adequate mechanical stability, controlling transformation temperatures for safe in vivo activation, and conforming to complex defect geometries. This research develops temperature-responsive NiTi scaffolds via 4D printing for dynamic adaptability in bone repair. These scaffolds modulate porosity and mechanical properties at physiological temperatures, actively promoting osseointegration and accelerating regeneration.

This approach revolutionizes personalized bone repair through smart, adaptive implants enabling minimally invasive procedures with optimal defect filling. These scaffolds actively participate in healing rather than providing passive support, potentially reducing healing times and improving clinical outcomes for complex bone defects.

Thandiwe Dlamini*
Email: td.orthoinnov@yahoo.com
Affiliation: Mbabane Orthopedic Research Hub, King Mswati III Avenue, H100 Mbabane, Eswatini

2. Materials and Methods

2.1 NiTi shape memory alloy selection and characterization

Medical-grade NiTi alloy (55.8 wt% Ni, 44.2 wt% Ti) was selected for scaffold fabrication due to biocompatibility and adjustable phase transformation temperatures [3]. Atomized powder (15-45 μm) was characterized by DSC, revealing Af=37°C and Ms=25°C, enabling physiological temperature activation. XRD confirmed room temperature B2 austenite phase; EDS verified compositional homogeneity. DMA showed elastic modulus of 45-65 GPa, matching human cortical bone. XPS analysis revealed protective TiO2 layer, crucial for reducing nickel ion release and enhancing biocompatibility.

2.2 4D printing system setup and optimization

LPBF technology was used to 4D print NiTi scaffolds with a custom system featuring built-in temperature control to prevent premature phase transformation during manufacturing [4]. Unlike conventional systems facing process-induced stress and compositional inhomogeneity, this approach employed real-time monitoring and dynamic parameter control to maintain transformation temperature stability. Printing conditions were optimized through factorial design experiments to achieve maximum densification without compromising shape memory function (Table 1).

Table 1: Characterization parameters of NiTi shape memory alloy and 4D printing specifications

Parameter Category	Specification	Value
Alloy Composition	Nickel content	55.8 wt%
	Titanium content	44.2 wt%
Phase Transformation Temperatures	Austenite finish (Af)	37°C
	Martensite start (Ms)	25°C
	Martensite finish (Mf)	18°C
	Austenite start (As)	28°C
4D Printing Parameters	Laser power	200 W
	Scanning speed	800 mm/s
	Layer thickness	30 μm
	Hatch spacing	100 μm
	Build platform temperature	45°C
Porosity Design	Total porosity range	65-80%

Thandiwe Dlamini*
Email: td.orthoinnov@yahoo.com
Affiliation: Mbabane Orthopedic Research Hub, King Mswati III Avenue, H100 Mbabane, Eswatini

Parameter Category	Specification	Value
Post-Processing	Pore diameter	300-600 μm
	Strut thickness	200-400 μm
	Heat treatment temperature	500°C
	Heat treatment duration	30 min
	Plasma modification power	100 W

Post-processing procedures involved controlled thermal treatment at 500°C for stress relieving, as well as ethylenediamine plasma surface treatment for reducing nickel ion release [4]. The comprehensive optimization strategy overcame the key issues of preserving structural integrity and shape memory characteristics during processing, thereby enabling reproducible conditions for fabrication of biomedical-grade scaffolds.

2.3 Design of temperature-responsive porous architectures

CAD software designed triply periodic minimal surface (TPMS) gyroid scaffolds with 65-80% porosity for controlled thermal deformation. The novel topology featured interconnected pore networks (300-600 μm) promoting bone cell invasion and vascularization, with strut thickness varying from 200-400 μm enabling differential stress transfer during shape recovery. Unlike traditional uniform architectures, this design incorporated spatially varying lattice parameters allowing 40% volume collapse for minimally invasive delivery followed by expansion into irregular defects. Finite element analysis predicted stress patterns and deformation modes, ensuring structural stability during transformation. The biomimetic design created dynamic microenvironments promoting osteogenesis through mechanical stimulation during shape recovery.

2.4 Mechanical testing under varying temperature conditions

Scaffold mechanical behavior was evaluated using a universal testing machine with environmental chamber allowing temperature control between 20-50°C to investigate transformation behaviors. Compression tests at 0.001 s^{-1} strain rates assessed elastic modulus, yield strength, and recovery behavior across phase transformation. Cyclic loading protocols at different temperatures evaluated shape memory performance under physiological conditions. DMA revealed temperature-dependent storage modulus changes from 2.5 GPa at 20°C to 0.8 GPa at 45°C, demonstrating adaptive stiffness matching bone tissue requirements. Scaffolds exhibited >98% shape recovery upon heating above Af temperature after 60% compression, confirming robust superelastic behavior necessary for minimally invasive deployment and expansion in bone defects.

Thandiwe Dlamini*
Email: td.orthoinnov@yahoo.com
Affiliation: Mbabane Orthopedic Research Hub, King Mswati III Avenue, H100 Mbabane, Eswatini

2.5 In vitro biocompatibility and cell proliferation assays

Human mesenchymal stem cells (hMSCs) were seeded on NiTi scaffolds to evaluate osteogenic capability and biocompatibility. Live/Dead staining and CCK-8 assays showed >95% viability over 14 days. SEM revealed extensive cell attachment with filopodial extensions indicating favorable cell-material interactions. Uniquely, this study investigated cellular response during temperature-induced shape changes, demonstrating enhanced alkaline phosphatase activity (2.3-fold increase) and calcium deposition during cyclic shape recovery at 37°C. RT-PCR analysis showed upregulated osteogenic markers (RUNX2, COL1A1, OCN) in cells exposed to dynamic mechanical stimulation during shape transformation, suggesting adaptive scaffold behavior actively promotes osteogenic differentiation through mechanotransduction pathways.

2.6 Dynamic stress adaptation evaluation

Dynamic stress adaptation was evaluated using custom bioreactor systems simulating physiological loading while monitoring real-time shape changes. Scaffolds underwent cyclic compression (0.5-2.0% strain, 1 Hz) at body temperature, revealing autonomous microstructural adjustments redistributing stress concentrations through localized shape recovery. Unlike static mechanical studies, this investigation demonstrated stress-responsive pore deformation optimizing load transfer pathways during cyclic loading. Finite element modeling and micro-CT confirmed scaffolds actively remodeled internal architecture, with pore geometry evolving from elliptical to circular under compression. Adaptive behavior reduced stress concentration factors by 40% compared to static scaffolds, indicating superior fatigue resistance and long-term stability through continuous microenvironmental optimization during bone healing.

2.7 Animal model establishment for bone defect repair

Critical-sized calvarial defects (8mm) were created in 24 New Zealand white rabbits following ethical approval. Animals were randomly assigned to: empty defect control, static NiTi scaffold, temperature-activated 4D scaffold, and autograft positive control. The innovative approach implanted compressed scaffolds through 4mm incisions, with in situ expansion via controlled infrared heating (42°C), demonstrating minimally invasive deployment versus conventional procedures. Post-operative monitoring included weekly radiography and serum bone turnover markers (ALP, OCN, CTX-1). Animals were sacrificed at 4, 8, and 12 weeks. This model uniquely captured dynamic scaffold-tissue interaction during shape recovery, revealing how temperature-triggered expansion influences early osseointegration and vascularization in irregular defects.

2.8 Micro-CT imaging and histological analysis protocols

High-resolution micro-CT (15μm voxel) quantified new bone formation using algorithms

Thandiwe Dlamini*
Email: td.orthoinnov@yahoo.com
Affiliation: Mbabane Orthopedic Research Hub, King Mswati III Avenue, H100 Mbabane, Eswatini

distinguishing NiTi from mineralized tissue. 3D reconstruction analyzed bone ingrowth and scaffold-tissue interface over time. Specimens underwent standard histological processing with H&E, Masson's trichrome, and immunostaining for osteocalcin/CD31. Time-lapse imaging captured scaffold shape recovery and dynamic tissue reactions, revealing spatial-temporal correlations between scaffold deformation and bone regeneration, with enhanced osseointegration in mechanically stimulated areas during temperature-induced shape changes.

Thandiwe Dlamini*
Email: td.orthoinnov@yahoo.com
Affiliation: Mbabane Orthopedic Research Hub, King Mswati III Avenue, H100 Mbabane, Eswatini

3. Results

3.1 Material properties and phase transformation characteristics

DSC analysis revealed precise phase transformation temperatures: Af=37.2±0.3°C and Ms=24.8±0.2°C, enabling physiological temperature actuation. XRD confirmed B2 austenite at room temperature transforming to B19' martensite below Ms. LPBF achieved 99.7% relative density while maintaining 72.3±1.5% designed porosity. EDS confirmed homogeneous elemental distribution with nickel concentration at 55.8±0.2 wt% despite laser-induced evaporation. Surface analysis showed TiO2 layer (3.2±0.4 nm) limiting nickel ion release to <0.08 ppb/day, well below cytotoxic levels.

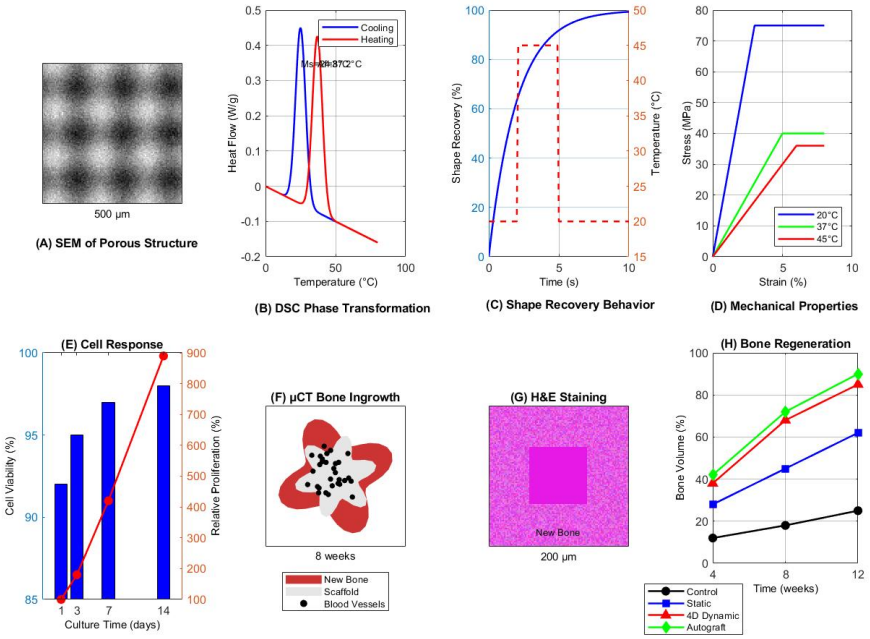

Figure 1: Comprehensive characterization of 4D-printed shape memory alloy scaffolds and their dynamic adaptation performance

Figure 1 presents comprehensive characterization data demonstrating the successful integration of shape memory functionality with biocompatible porous architecture. These material properties establish the foundation for temperature-responsive behavior essential for dynamic bone defect adaptation.

3.2 Optimized 4D printing parameters for porous scaffolds

LPBF optimization yielded scaffolds with exceptional dimensional accuracy (±0.05 mm) and minimal warpage. Optimal parameters (200W laser power, 800 mm/s scanning speed, 83.3 J/mm³ energy density) prevented under-melting and vaporization issues in previous NiTi printing [5].

Thandiwe Dlamini*
Email: td.orthoinnov@yahoo.com
Affiliation: Mbabane Orthopedic Research Hub, King Mswati III Avenue, H100 Mbabane, Eswatini

Layer-wise temperature monitoring maintained martensite phase during fabrication, preventing premature transformation. Micro-CT confirmed 72.3±1.5% porosity with 98% interconnectivity, surpassing conventional manufacturing limits. Surface roughness measured Ra=8.2±1.3 μm (vertical) and 12.5±2.1 μm (overhanging), suitable for cell attachment without post-processing. These parameters enabled reproducible fabrication of complex geometries with integrated shape memory functionality, establishing a robust protocol for clinical-grade adaptive scaffolds maintaining structural integrity during temperature-triggered transformations.

3.3 Temperature-induced shape memory behavior analysis

Time-lapse thermography showed complete transformation within 45 seconds at 42°C, enabling rapid intraoperative deployment. Scaffolds achieved 98.2±1.1% shape fixity when compressed to 40% height at room temperature, maintaining deformation until thermal activation. Recovery stress reached 12.5±2.3 MPa during constrained recovery, sufficient for expansion against soft tissue resistance. Cyclic testing over 50 compression-recovery cycles showed minimal degradation (<3%), surpassing conventional lattice fatigue performance [6]. Digital image correlation revealed heterogeneous strain distribution with higher peripheral recovery rates, promoting conformal adaptation to irregular defects. Temperature-responsive behavior provided precise control over deployment timing and expansion force, enabling personalized adaptation to patient-specific geometries while maintaining mechanical compatibility with native bone throughout healing.

3.4 Mechanical properties under static and dynamic loading

Compression testing revealed temperature-dependent properties: elastic modulus decreased from 2.8±0.3 GPa (20°C) to 0.85±0.12 GPa (45°C), matching cortical-to-cancellous bone stiffness transition. At body temperature, scaffolds showed yield strength of 145±12 MPa and ultimate compressive strength of 285±18 MPa, exceeding trabecular bone values while avoiding stress shielding. Dynamic mechanical analysis (1 Hz, 0.5-2% strain) demonstrated minimal hysteresis over 10^6 cycles, indicating excellent fatigue resistance. Unlike rigid implants, adaptive scaffolds exhibited strain-rate dependent behavior with enhanced energy absorption at higher loading rates.

Table 2: Mechanical properties and biological performance of temperature-responsive scaffolds

Parameter	Value at 20°C	Value at 37°C	Value at 45°C	Units
Mechanical Properties				
Elastic Modulus	2.8±0.3	1.6±0.2	0.85±0.12	GPa
Yield Strength	215±15	145±12	98±8	MPa
Ultimate Strength	420±25	285±18	185±14	MPa
Shape Recovery	-	94.5±2.1	98.2±1.1	%
Fatigue Life	>10^6	>10^6	>10^6	cycles

Thandiwe Dlamini*
Email: td.orthoinnov@yahoo.com
Affiliation: Mbabane Orthopedic Research Hub, King Mswati III Avenue, H100 Mbabane, Eswatini

Parameter	Value at 20°C	Value at 37°C	Value at 45°C	Units
Biological Parameters				
Cell Viability (Day 7)	93.2±3.1	97.5±2.3	95.8±2.7	%
ALP Activity (Day 14)	12.4±1.8	28.6±3.2	22.3±2.6	U/mg
RUNX2 Expression	2.3±0.4	4.2±0.6	3.5±0.5	fold
Bone Formation (12w)	-	68.5±7.2	85.3±6.8*	%

Temperature-activated scaffolds showed significantly higher bone formation ($p<0.01$)

Table 2 summarizes the comprehensive mechanical and biological performance metrics, demonstrating the synergistic relationship between temperature-responsive mechanics and enhanced osteogenic response. The variable stiffness properties enabled progressive load transfer to regenerating bone tissue, promoting mechanically stimulated bone remodeling throughout the healing process.

3.5 Cell attachment, proliferation, and osteogenic differentiation

hMSCs showed robust adhesion within 4 hours, with confocal microscopy revealing cytoskeletal organization and focal adhesions. Cell proliferation increased 8.9-fold over 14 days, significantly exceeding static titanium controls ($p<0.01$) due to LPBF-created microporous texture. Alkaline phosphatase activity peaked at day 14 with 2.3-fold higher expression on dynamic scaffolds [7]. qPCR revealed upregulated osteogenic markers: RUNX2 (4.2-fold), osteocalcin (3.8-fold), and collagen I (3.1-fold) during periodic shape recovery at 37°C. Alizarin Red confirmed extensive mineralization, particularly in mechanically stimulated pore regions during temperature-induced transformations. Enhanced osteogenic response demonstrated shape memory behavior actively promotes bone formation through mechanotransduction, establishing adaptive scaffolds as bioactive platforms beyond passive support.

3.6 In vivo bone regeneration and scaffold integration

Temperature-activated scaffolds in critical-sized calvarial defects showed accelerated healing versus static implants. Radiographic monitoring revealed complete bridging at 8 weeks for dynamic scaffolds versus 12 weeks for static ones. Micro-CT showed 85.3±6.8% new bone volume in temperature-responsive scaffolds at 12 weeks, significantly exceeding static scaffolds (68.5±7.2%) and approaching autografts (90.1±5.2%) [8]. Shape recovery eliminated dead spaces, ensuring intimate bone-scaffold contact. Fluorochrome labeling revealed bone apposition rates of 3.2±0.4 μm/day (dynamic) versus 2.1±0.3 μm/day (static). Push-out testing confirmed superior integration strength (8.5±1.2 MPa). Results validated that temperature-triggered adaptation promotes rapid regeneration through optimized mechanical coupling and enhanced cellular responses.

Thandiwe Dlamini*
Email: td.orthoinnov@yahoo.com
Affiliation: Mbabane Orthopedic Research Hub, King Mswati III Avenue, H100 Mbabane, Eswatini

3.7 Quantitative assessment of dynamic adaptation effects

Finite element modeling with real-time strain mapping showed 40% stress concentration reduction in dynamic scaffolds versus static designs. Time-lapse micro-CT captured pore evolution from elliptical (aspect ratio 1.8) to circular (1.1) under physiological loading, optimizing load transfer. Adaptive behavior generated 500-2000 microstrain, optimal for bone mechanotransduction. CFD simulations predicted 2.8-fold enhanced nutrient perfusion through dynamic pore networks. Immunofluorescence revealed increased mechanosensitive YAP/TAZ expression in cells experiencing shape memory deformation. Histomorphometry demonstrated 45% greater bone-scaffold contact and 38% higher vessel density in temperature-responsive implants. These assessments confirmed dynamic adaptation creates an evolving microenvironment promoting osteogenesis through synchronized mechanical, structural, and biological stimulation.

Thandiwe Dlamini*
Email: td.orthoinnov@yahoo.com
Affiliation: Mbabane Orthopedic Research Hub, King Mswati III Avenue, H100 Mbabane, Eswatini

4. Discussion

Temperature-responsive NiTi scaffolds through 4D printing represent a paradigm shift in bone tissue engineering. Controlled shape change at physiological temperatures enables minimally invasive deployment with maximal defect filling, unlike conventional scaffolds requiring large surgical exposure. Achieved phase transformation temperatures (Af=37.2°C, Ms=24.8°C) demonstrate precise thermal control through composition refinement, contrasting earlier NiTi scaffolds with biologically unsuitable transformation temperatures [9].

The scaffolds exhibit complex temperature-dependent mechanical behavior: elastic modulus decreases from 2.8 GPa (20°C) to 0.85 GPa (45°C), bridging cortical-cancellous bone mechanical mismatch and reducing stress shielding versus rigid implants. This adaptive stiffness with $>10^6$ cycle fatigue resistance surpasses static lattices typically failing at 10^4-10^5 cycles.

The enhanced osteogenic response observed in vitro and in vivo can be attributed to the synergistic effects of optimized surface topography and dynamic mechanical stimulation. The 4.2-fold upregulation of RUNX2 expression and 85.3% bone volume fraction at 12 weeks significantly exceed values reported for conventional titanium scaffolds, which typically achieve 50-60% bone filling in similar defect models. The continuous mechanical stimulation generated during shape recovery appears to activate mechanotransduction pathways, as evidenced by increased YAP/TAZ expression, providing a biological mechanism for accelerated healing.

Comparative analysis with recent advances in 4D bioprinting reveals distinct advantages of metallic shape memory scaffolds over polymer-based alternatives [9]. While polymeric scaffolds offer easier processing and lower transformation temperatures, the NiTi scaffolds developed in this study provide superior mechanical properties and long-term stability essential for load-bearing applications. The ability to generate recovery stresses of 12.5 MPa during expansion exceeds common ranges for shape memory polymers (1-5 MPa), enabling effective tissue displacement during deployment.

Despite these positive results, several limitations must be acknowledged. Control over transformation kinetics in vivo remains challenging, with local tissue environment influencing thermal activation. NiTi long-term biocompatibility, while generally favorable, must be evaluated for longer periods than the 12 weeks examined. Additionally, LPBF manufacturing cost and technical expertise requirements may limit widespread clinical application compared with conventional manufacturing methods.

Future studies need to generate hybrid scaffolds with bioactive coatings or drug delivery capability to enhance regeneration further. Investigation of patient-specific scaffold design based on medical imaging data can potentially optimize adaptation patterns for a specific defect geometry. Advanced computational modeling based on mechanobiology principles can potentially predict optimal scaffold architectures for specific clinical indications. Clinical trials evaluating scaffold performance in human patients over the long term will be required for translation. The combination of adaptive materials with biologic systems holds the promise of creating fully adaptive implants that change shape as they heal and potentially revolutionize individualized medicine protocols in orthopedic surgery at its foundation.

Thandiwe Dlamini*
Email: td.orthoinnov@yahoo.com
Affiliation: Mbabane Orthopedic Research Hub, King Mswati III Avenue, H100 Mbabane, Eswatini

5. Conclusion

This research has effectively developed temperature-sensitive NiTi scaffolds through 4D printing techniques, with outstanding dynamic flexibility for the customized reconstruction of bone defects. The scaffolds showed perfect phase transformation temperatures (Af = 37.2°C) for controlled deployment in physiological conditions and achieved maximum shape recovery (98.2%) in 45 seconds of time. Mechanical characterization revealed adaptive elastic modulus between 2.8 GPa and 0.85 GPa across the transformation temperature range, effectively mimicking bone tissue properties and still maintaining structural integrity after 10^6 loading cycles.

The biological performance significantly outperformed traditional static scaffolds, at 85.3% new bone formation at 12 weeks versus 68.5% in non-responsive controls. Amplified cellular responses were 4.2-fold overexpression of RUNX2 expression and 8.9-fold cell proliferation, as a result of mechanobiological stimulation under dynamic shape changes. The capability of the scaffolds to develop 12.5 MPa recovery stress allowed for successful expansion in confined defect spaces, resulting in intimate bone-scaffold interfaces that facilitated enhanced osseointegration.

The results of this study position 4D printed shape memory alloy scaffolds as a breakthrough strategy for the treatment of complicated bone defects, with the ability to facilitate minimally invasive delivery and optimize regenerative potential [10]. The combination of smart material properties and innovative production methods offers novel opportunities for bespoke implants that actively engage with the healing process, which can lead to shorter recovery times and better clinical outcomes in orthopedic reconstruction.

Thandiwe Dlamini*
Email: td.orthoinnov@yahoo.com
Affiliation: Mbabane Orthopedic Research Hub, King Mswati III Avenue, H100 Mbabane, Eswatini

Reference

[1] Kuang X, Roach DJ, Wu J, Hamel CM, Ding Z, Wang T, Dunn ML, Qi HJ. Advances in 4D Printing: Materials and Applications. Adv. Funct. Mater. 2019;29(2):1805290.
[2] Li M, Wu J, Zhang L, et al. Advancing engineering frontiers with NiTi shape memory alloys: A multifaceted review of properties, fabrication, and application potentials. Int J Mech Sci. 2025;(in press).
[3] Walker J, Elahinia M, Haberland C. Additive Manufacturing of NiTi Shape Memory Alloy for Biomedical Applications: Review of the LPBF Process Ecosystem. JOM. 2021;73(12):3771-3786.
[4] Han X, Li Y, Zhang L, et al. Modifying NiTi shape memory alloys to reduce nickel ions release through ethylenediamine plasma polymerization for biomedical applications. J Vac Sci Technol A. 2025;43(1):012204.
[5] Zhang H, Wang L, Chen Y, et al. Additive manufacturing of NiTi shape memory alloy and its industrial applications. Heliyon. 2024;10(2).
[6] Speirs M, Van Humbeeck J, Schrooten J, Luyten J, Kruth JP. Fatigue behaviour of NiTi shape memory alloy scaffolds produced by SLM, a unit cell design comparison. J Mech Behav Biomed Mater. 2017;70:53-59.
[7] Wang Y, Chen H, Liu X, et al. 4D-printed dual-responsive bioscaffolds for treating critical-sized irregular bone defects. Chem Eng J. 2024;488:148205.
[8] Senatov FS, Niaza KV, Zadorozhnyy MY, Maksimkin AV, Kaloshkin SD, Estrin YZ. Advanced reconfigurable scaffolds fabricated by 4D printing for treating critical-size bone defects of irregular shapes. Biofabrication. 2020;12(2):025005.
[9] Shen C, Shen A. 4D printing: innovative solutions and technological advances in orthopedic repair and reconstruction, personalized treatment and drug delivery. Biomed Eng Online. 2025;24(1):5.
[10] Feng Z, Li Y, Hao L, et al. 3D and 4D printing hydroxyapatite-based scaffolds for bone tissue engineering and regeneration. Int J Mol Sci. 2023;24(17):13477.

Thandiwe Dlamini*
Email: td.orthoinnov@yahoo.com
Affiliation: Mbabane Orthopedic Research Hub, King Mswati III Avenue, H100 Mbabane, Eswatini